

Scaling the leaf length-times-width equation to predict total leaf area of shoots

Kohei Koyama^{1,*} and Duncan D. Smith²¹Department of Agro-environmental Science, Obihiro University of Agriculture and Veterinary Medicine, Inadacho, Obihiro, Hokkaido 080-8555, Japan and ²Department of Botany, University of Wisconsin—Madison, 430 Lincoln Dr., Madison, WI 53706, USA* For correspondence. E-mail: koyama@obihiro.ac.jp

Received: 6 February 2022 Returned for revision: 17 March 22 Editorial decision: 18 March 2022 Accepted: 24 March 2022

- **Background and Aims** An individual plant consists of different-sized shoots, each of which consists of different-sized leaves. To predict plant-level physiological responses from the responses of individual leaves, modelling this within-shoot leaf size variation is necessary. Within-plant leaf trait variation has been well investigated in canopy photosynthesis models but less so in plant allometry. Therefore, integration of these two different approaches is needed.
- **Methods** We focused on an established leaf-level relationship that the area of an individual leaf lamina is proportional to the product of its length and width. The geometric interpretation of this equation is that different-sized leaf laminas from a single species share the same basic form. Based on this shared basic form, we synthesized a new length-times-width equation predicting total shoot leaf area from the collective dimensions of leaves that comprise a shoot. Furthermore, we showed that several previously established empirical relationships, including the allometric relationships between total shoot leaf area, maximum individual leaf length within the shoot and total leaf number of the shoot, can be unified under the same geometric argument. We tested the model predictions using five species, all of which have simple leaves, selected from diverse taxa (Magnoliids, monocots and eudicots) and from different growth forms (trees, erect herbs and rosette herbs).
- **Key Results** For all five species, the length-times-width equation explained within-species variation of total leaf area of a shoot with high accuracy ($R^2 > 0.994$). These strong relationships existed despite leaf dimensions scaling very differently between species. We also found good support for all derived predictions from the model ($R^2 > 0.85$).
- **Conclusions** Our model can be incorporated to improve previous models of allometry that do not consider within-shoot size variation of individual leaves, providing a cross-scale linkage between individual leaf-size variation and shoot-size variation.

Key words: Allometry, scaling, leaf size, shoot size, intraspecific, Corner's rule, self-affine, *Cardiocrinum cordatum*, *Fallopia sachalinensis*, *Magnolia kobus*, *Prunus sargentii*, *Ulmus davidiana* var. *japonica*.

INTRODUCTION

Plants are modular organisms, and they can be considered as a population of leaves and stems (Harper and Bell, 1979). Within each plant, organs (e.g. leaf or stem) usually differ in size, physiology and microenvironments (Field, 1983; DeJong *et al.*, 1989; Koyama and Kikuzawa, 2010; Niinemets, 2016; Kusi and Karsai, 2020; Maslova *et al.*, 2021). Therefore, photosynthesis of individual plants or ecosystems has been modelled as the sum of those of individual leaves (Bazzaz and Harper, 1977; Field, 1983; Ackerly and Bazzaz, 1995; Koyama and Kikuzawa, 2009). This cross-scale relationship between organ-level and plant- or ecosystem-level physiology has long been recognized as one of the central issues in canopy photosynthesis models (Field, 1991; Hikosaka *et al.*, 2016; Niinemets, 2016).

However, despite its importance, within-canopy or within-plant variation of organs has rarely been incorporated in the field of plant allometry. Allometry (i.e. power functions) has been a successful tool for analysing relationships between the properties of different-sized individual plants or organs (Niklas,

1994; Enquist *et al.*, 2009; Mori *et al.*, 2010; Savage *et al.*, 2010; Bentley *et al.*, 2013; Okie, 2013; Banavar *et al.*, 2014; Huang *et al.*, 2019; Lin *et al.*, 2020; Olson *et al.*, 2020; Kurosawa *et al.*, 2021; Wang *et al.*, 2021). However, most plant-level allometric models are based on the simplifying assumption that each individual plant has terminal organs (twigs or leaves) of the same size (Enquist *et al.*, 2009; West *et al.*, 2009; Savage *et al.*, 2010; Banavar *et al.*, 2014). These approaches contrast with organ-level studies on the within-plant size variation of twigs and leaves (Dombroskie and Aarssen, 2012; Koyama *et al.*, 2012, 2017; Kusi and Karsai, 2020; Maslova *et al.*, 2021). The integration of these two approaches, plant allometry and canopy photosynthesis models, has not been achieved yet, although both approaches independently predict plant- or ecosystem-level metabolism (Koyama *et al.*, 2017).

Here, a shoot is defined as a terminal single current-year stem with all its appendages (leaves, buds, flowers, fruits, etc.). A shoot is equivalent to an individual ramet (i.e. whole above-ground part of a plant) in single-stem herbaceous species. For trees, a shoot is a fundamental unit of growth (Sterck *et al.*, 2005; Sterck and Schieving, 2007; Lecigne *et al.*, 2021)

and reproduction (Chen *et al.*, 2009; Scott and Aarssen, 2013; Miranda *et al.*, 2019; Fajardo *et al.*, 2020). Given its importance, allometric relationships of shoot size and total shoot leaf area have been important topics in plant ecophysiology (Corner, 1949; White, 1983; Ackerly and Donoghue, 1998; Brouat *et al.*, 1998; Westoby and Wright, 2003; Kleiman and Aarssen, 2007; Olson *et al.*, 2009, 2018; Sun *et al.*, 2010, 2020; Yan *et al.*, 2013; Trueba *et al.*, 2016; Fan *et al.*, 2017; Smith *et al.*, 2017; Zhu *et al.*, 2019; Fajardo *et al.*, 2020). However, most previous studies on leaf vs. shoot size allometry have focused on the relationship among shoot size, total shoot leaf area, total leaf number and/or mean individual leaf size on the shoot. These studies are not mutually exclusive of, but do not yet have a theoretical connection with, the fact mentioned above that a shoot has a population of leaves with a size distribution (see Bazzaz and Harper, 1977). Because the total leaf area of a shoot (or a plant) is the sum of the areas of individual leaves, the leaf size distribution within a shoot is one of the main determinants of whole-plant or total shoot leaf area (Seleznayova and Greer, 2001; Bultynck *et al.*, 2004). Yet, with only a few exceptions (e.g. Koyama *et al.*, 2012; Smith *et al.*, 2017), this fact was not considered in most previous studies on leaf size – shoot size allometry (e.g. Sun *et al.*, 2006, 2010, 2017, 2019a, b, 2020; Kleiman and Aarssen, 2007; Ogawa, 2008; Yang *et al.*, 2008, 2009, 2010; Milla, 2009; Xiang *et al.*, 2009a, 2010; Whitman and Aarssen, 2010; Dombroskie and Aarssen, 2012; Scott and Aarssen, 2012, 2013; Yan *et al.*, 2013; Dombroskie *et al.*, 2016; Trueba *et al.*, 2016; Olson *et al.*, 2018; Miranda *et al.*, 2019; Zhu *et al.*, 2019; Fajardo *et al.*, 2020).

Therefore, the objective of this study was to clarify the relationship between size variations at two different levels: the within-species size variation of shoots and the within-shoot size variation of leaves. We propose a simple geometric model that incorporates these two size variations. The model is a mathematical quantification and generalization of the results of Koyama *et al.* (2012), which showed that differently sized plants of the herbaceous species *Cardiocrinum cordatum* share the same basic structure. However, their study did not provide a mathematical model that could derive these relationships. Furthermore, the present model is more general than the findings of Koyama *et al.* (2012), in that it can be applied to various plant forms (trees, rosettes and erect herbs). In the present model, maximum leaf size within a shoot plays a pivotal role. In relation to this, Sun *et al.* (2019a, 2020) recently proposed a model that unified previous studies on the leaf size–number trade-off (Kleiman and Aarssen, 2007), shoot photosynthesis and growth (Niklas and Enquist, 2001, 2002), and stem cross-sectional area [i.e. pipe model (Shinozaki *et al.*, 1964; Brouat *et al.*, 1998)]. Sun *et al.* (2019a, 2020) also found that maximum leaf size within a shoot is a major determinant of the leaf number per stem mass across different species. Moreover, Lopes and Pinto (2005), and Heerema, Spann, and their colleagues (Heerema *et al.*, 2008; Spann and Heerema, 2010) proposed empirical relationships that use maximum leaf size to predict total shoot leaf area. Nonetheless, all of these previous findings, specifically on the usefulness of maximum leaf size, are phenomenological because they do not provide any quantitative model to explain why maximum leaf size is a predictor of the total leaf area of a shoot. Here, we used an entirely novel approach, which uses maximum leaf size to model within-shoot and between-shoot leaf size variations.

MODEL

Individual leaf area (A_{leaf}) is defined as the area of one side of each lamina (i.e. leaf blade) (John *et al.*, 2017). A shoot may have one or multiple leaves, each of which may differ in size. Therefore, the total leaf area of a shoot (A_{shoot}) is defined as the sum of A_{leaf} of all the leaves on that shoot:

$$A_{\text{shoot}} \equiv \sum_{\text{shoot}} A_{\text{leaf}} \quad (1)$$

The symbol ‘ \equiv ’ indicates ‘defined as’. As our aim was to find simple formulas that predict A_{shoot} , taking into consideration the within-shoot size variation of A_{leaf} , the present model is based on several simplifications. (1) We focused only on the leaf laminas that determine A_{shoot} . We thus ignored any other organs (e.g. stem, petioles, buds and reproductive organs). (2) Our model only deals with simple leaves with flat-shaped laminas: the current model cannot be applied to leaves of different forms (e.g. compound leaves that consist of multiple leaflets, succulent leaves or conifer needles). The limitations associated with these simplifications will be addressed in the Discussion.

We use the two words ‘similar’ and ‘affine’ (Fig. 1), which have been used as compound words ‘self-similar’ and ‘self-affine’ in fractal geometry (Falconer, 2003; Okie, 2013; Shi *et al.*, 2021b). In Fig. 1, in each panel (A and B), the two green triangles represent two different-sized individual leaf laminas. Two shapes are similar if they can be made identical by multiplying each dimension by a single constant (i.e. similar transformation). Two shapes are affine if they can be made identical by multiplying each dimension by a different constant (i.e. affine transformation).

First, we focused on individual leaves. Within a species, the area of an individual leaf (A_{leaf}) is proportional to the lamina length (L_{leaf}) times lamina width (W_{leaf}) (Cain and Castro, 1959; Teobaldelli *et al.*, 2019a, b; Yu *et al.*, 2020; Huang *et al.*, 2021; Li *et al.*, 2021; Schrader *et al.*, 2021; Shi *et al.*, 2021a) (Fig. 2A):

$$A_{\text{leaf}} \propto L_{\text{leaf}} \times W_{\text{leaf}} \quad (2)$$

The symbol ‘ \propto ’ indicates ‘proportional to’. Equation (2) is known as the Montgomery equation (Yu *et al.*, 2020; Shi *et al.*, 2021a). It indicates that leaves from the same species are affine to each other.

Next, we extend eqn (2) to the level of shoots to predict A_{shoot} . We hypothetically detach all the leaf laminas from the stem,

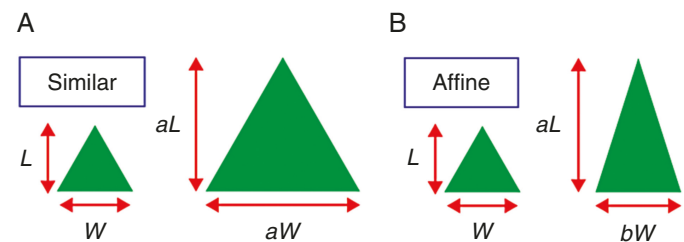


FIG. 1. Definition of the words ‘similar’ and ‘affine’ used in this article. (A) Two similar triangles share the same length-to-width ratio. (B) Two affine triangles may have different length-to-width ratios. For an affine transformation to change the small triangle into the large triangle, the scaling factor in one direction (a) is not necessarily equal to that in the other direction (b), and similar transformation is a special case of affine transformation when $a = b$. In both cases, the area is proportional to the product of the length (L) and width (W).

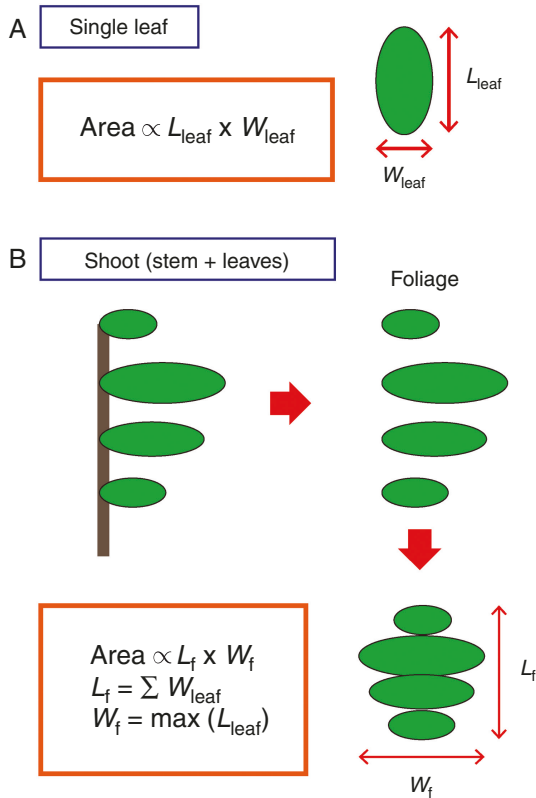


FIG. 2. The length-times-width model for (A) an individual leaf and (B) a shoot.

and place them side-by-side on a flat plane to determine its dimensions as illustrated in Fig. 2B:

$$\begin{cases} L_f \equiv \sum_{\text{shoot}} W_{\text{leaf}} \\ W_f \equiv \max_{\text{shoot}} (L_{\text{leaf}}) \end{cases} \quad (3)$$

We refer to this set of leaf laminae as the ‘foliage’ of each shoot. The subscripts ‘f’ in eqn (3) stand for ‘foliage’. We exclude petioles because they contribute to the 3D arrangement with relatively little contribution to A_{shoot} . The utility of rearranging the leaves is that both foliage length (L_f) and foliage width (W_f) can be defined independently from the 3D arrangement of the leaves. Our main hypothesis is that, within a single species, different-sized sets of foliage are affine, as is the case of individual leaves. This indicates that the total area of a foliage (which is A_{shoot} , by definition) is proportional to the product of L_f and W_f (Fig. 2B):

$$A_{\text{shoot}} \propto L_f \times W_f \quad (4)$$

We will call eqn (4) the ‘foliage length-times-width equation’. Note that foliage length (L_f) is defined using leaf width (not leaf length), and foliage width (W_f) is defined using leaf length. The reason for these definitions is that both ‘leaf length’ and ‘foliage length’ are defined in the proximal–distal direction. In other words, foliage is analogous to a pinnately compound leaf that extends from the parent stem in the distal direction.

Next, we compare different-sized shoots from a single species. As shoot size increases, both L_f and W_f increase. We assume that the ratio of the relative growth rates of the foliage in these two directions is constant (Huxley, 1932; Niklas, 1994; Okie, 2013), and therefore follows the allometric relationship:

$$L_f \propto W_f^\beta \quad (\beta > 1) \quad (5)$$

The exponent β is expected to be >1 , for the following reason. If foliage always consists of a single leaf, irrespective of its size, by definition L_f and W_f are equivalent to W_{leaf} and L_{leaf} , respectively. In this case, L_f and W_f should be approximately proportional to each other (i.e. $\beta \approx 1$). However, in reality, a shoot usually has multiple leaves. Because L_f is defined as the sum of the widths of *all* leaves, larger foliage with more leaves should have a disproportionately larger length relative to its width than small foliage ($\beta > 1$). In general, the value of β may vary among species, depending on the species’ intrinsic maximum leaf size and leafing intensity. In the Results, we show that eqn (5) is valid. Before demonstrating this, we proceed by assuming that eqn (5) is valid to derive other predictions. By combining eqns (4) and (5), we obtained:

$$A_{\text{shoot}} \propto W_f^{\beta+1} \equiv \left[\max_{\text{shoot}} (L_{\text{leaf}}) \right]^{\beta+1} \quad (6)$$

As mentioned above, the lamina area of an individual leaf is predicted by the product of lamina length and width with high accuracy (i.e. high R^2 values). Additionally, it is known that individual leaf area can also be predicted by a quadratic function of lamina length or width alone [e.g. $A_{\text{leaf}} \propto (L_{\text{leaf}})^2$], albeit with less accuracy (Teobaldelli *et al.*, 2019a, b). Similarly, eqn (6) predicts that A_{shoot} can also be predicted by W_f alone, with less but acceptable accuracy. Note that because $\beta > 1$, the exponent is expected to be >2 . Suppose we further use an empirical relationship that individual lamina length is approximately proportional to lamina width [$L_{\text{leaf}} \propto W_{\text{leaf}}$ (Ogawa *et al.*, 1995)], by using eqn (6), we predicted that the maximum leaf lamina width within a shoot can also be used as a predictor of A_{shoot} :

$$A_{\text{shoot}} \propto \left[\max_{\text{shoot}} (W_{\text{leaf}}) \right]^{\beta+1} \quad (7)$$

These predictions [eqns (6) and (7)] were also tested in this study. Previous studies have already recognized the usefulness of maximum leaf size as a predictor of A_{shoot} (Lopes and Pinto, 2005; Heerema *et al.*, 2008; Sun *et al.*, 2019a; Teobaldelli *et al.*, 2020). However, these studies used maximum leaf size only as empirical models. Therefore, none of them has provided a quantitative theory that explains why this relationship holds. In the following subsections, we show that these empirical relationships can also be derived as corollaries of the present model.

Sun *et al.*’s equation

Sun *et al.* (2019a, 2020) found that A_{shoot} is proportional to the product of the maximum leaf area and total number of leaves on each shoot (N), because the maximum individual leaf area of a shoot corresponds to its potential leaf-producing capacity. This relationship can also be derived from our model (see Appendix for derivation):

$$A_{\text{shoot}} \propto N \cdot \max_{\text{shoot}} (A_{\text{leaf}}) \quad (8)$$

We retest this prediction in this study.

Size-number allometry

We also derived the allometric relationship between A_{shoot} and the total number of leaves on each shoot (N) reported by Koyama *et al.* (2012) (see Appendix for derivation):

$$A_{\text{shoot}} \propto N^\alpha, \quad \text{where } \alpha \equiv \frac{\beta + 1}{\beta - 1} = 1 + \frac{2}{\beta - 1} > 1 \quad (\because \beta > 1) \quad (9)$$

Generally, the exponent α may vary depending on species as a function of β . The predicted allometric relationship between A_{shoot} and N with the exponent $\alpha > 1$ (given $\beta > 1$) agrees with the empirical result reported by Koyama *et al.* (2012). We retested this prediction in this study. In addition, eqn (9) can be rearranged to predict the scaling relationship between mean individual leaf area ($=A_{\text{shoot}}/N$) and A_{shoot} with the exponent $0 < \lambda < 1$ (see Appendix for derivation):

$$\frac{A_{\text{shoot}}}{N} \propto (A_{\text{shoot}})^\lambda, \quad \text{where } \begin{cases} \lambda \equiv 1 - \frac{1}{\alpha} = \frac{2}{\beta + 1} \\ 0 < \lambda < 1 \quad (\because \beta > 1) \end{cases} \quad (10)$$

The prediction that $0 < \lambda < 1$ was empirically supported by Smith *et al.* (2017).

Heerema–Spann–Teobaldelli *et al.*'s equation

Heerema, Spann and their colleagues (Heerema *et al.*, 2008; Spann and Heerema, 2010) reported an empirical relationship that A_{shoot} can be predicted by the maximum leaf length of a shoot (i.e. foliage width, W_f) and the total number of leaves on that shoot (N) using woody fruit crop species. Teobaldelli *et al.* (2020) modified this relationship into a general allometric form. These relationships can also be derived from our model (see Appendix for derivation):

$$A_{\text{shoot}} \propto W_f \cdot N^\gamma, \quad \text{where } \begin{cases} \gamma \equiv \frac{\beta}{\beta - 1} = 1 + \frac{1}{\beta - 1} \\ \gamma > 1 \quad (\because \beta > 1) \end{cases} \quad (11)$$

Equation (11) was proposed as an empirical model by Teobaldelli *et al.* (2020), which includes the formula proposed by Heerema, Spann and their colleagues as a specific case when $\gamma = 1$, which does not take into consideration the β -dependency of γ . Generally, γ may vary among species as a function of β . Here, eqn (11) was tested by the following allometric relationship:

$$\frac{A_{\text{shoot}}}{W_f} \propto N^\gamma \quad (12)$$

We also directly tested eqn (12). Unlike eqns (4) and (5), eqn (12) does not use foliage length (L_f) as a variable, and therefore eqn (12) can be tested independently.

Lopes–Pinto's equation

Lopes and Pinto (2005) found an empirical formula that predicts A_{shoot} for a wine grape variety using the maximum and

minimum leaf area within each shoot. They found that each shoot's mean individual leaf area can be estimated as the mean of maximum and minimum leaf area within that shoot. This relationship can also be derived from our model (see Appendix for derivation):

$$A_{\text{shoot}} = k \cdot N \left[\frac{\min_{\text{shoot}} (A_{\text{leaf}}) + \max_{\text{shoot}} (A_{\text{leaf}})}{2} \right] \quad (13)$$

The symbol k is a proportionality constant. Lopes, Pinto and colleagues (Lopes and Pinto, 2005; Phinopoulos *et al.*, 2015) found the same relationship as eqn (13) for two wine grape varieties as an empirical formula. They used an empirical value of $k = 1$ (i.e. in their cases, mean individual leaf area was simply the average value of the largest and the smallest leaves) as a specific value for the grape varieties. Generally, k may vary depending on the species (depending on the arrangement of different-sized leaves along a shoot). This prediction was also tested in this study.

MATERIALS AND METHODS

Study species

The study species and the sample sizes are listed in Table 1. Each species is referred to by its genus name after its first mention. All species have simple leaves with reticulate or reticulate-like venation patterns. (1) Kobushi magnolia (*Magnolia kobus*, Magnoliaceae). *Magnolia* was selected because it is taxonomically separate from the other species (APG IV, 2016). (2) *Cardiocrinum cordatum* (including var. *glehnii*) (Liliaceae) is a monocarpic perennial herb. This species belongs to the monocots (APG IV, 2016), but its leaves have reticulate venation patterns that are similar to those of eudicots (see photographs in Koyama *et al.*, 2012). Small individual plants form rosettes on the ground without elongating their stems, whereas large plants become bolting rosettes, which elongate their vertical stems with flower buds on top (Ohara *et al.*, 2006; Komamura *et al.*, 2021). (3) Sargent's cherry (*Prunus sargentii*, Rosaceae) and (4) Japanese elm (*Ulmus davidiana* var. *japonica*, Ulmaceae). *Prunus* and *Ulmus* were chosen as typical broadleaved deciduous trees in temperate forests. (5) Giant knotweed (*Fallopia sachalinensis*, Polygonaceae) is a high-stature erect herb (plant height often reaches 2–3 m) with large leaves along its vertical stem. *Cardiocrinum* and *Fallopia* were chosen because they have contrasting growth forms (rosette vs. erect) and are from different taxonomic groups (monocot vs. eudicot).

Field sampling

A shoot is defined herein as a single current-year stem with its appendages (leaves, buds, flowers, fruits, etc.). For the two single-stemmed herbaceous species (*Cardiocrinum* and *Fallopia*), a shoot is equivalent to an entire above-ground part of an individual ramet, and therefore A_{shoot} is equivalent to whole-plant leaf area. Sample sizes and the sampling locations are given in Table 1. Sampling was conducted in summer (June–August) in 2016 and 2020. All sampling sites were located in Obihiro City or the adjacent Otofuke Town in Hokkaido Island

TABLE 1. Study species and sample sizes

	<i>Magnolia kobus</i>	<i>Cardiocrinum cordatum</i>	<i>Prunus sargentii</i>	<i>Ulmus davidiana</i> var. <i>japonica</i>	<i>Fallopia sachalinensis</i>
Taxonomy	Magnoliid (Magnoliales, Magnoliaceae)	Monocot (Liliales, Liliaceae)	Eudicot (Rosales, Rosaceae)	Eudicot (Rosales, Ulmaceae)	Eudicot (Caryophyllales, Polygonaceae)
Growth form	Tree (deciduous)	Herb (rosette or bolting)	Tree (deciduous)	Tree (deciduous)	Erect herb
Location	R, T	F, H	U	U, F	U
Number of shoots investigated	37	36	39	43	29
Size ranges A_{shoot} (cm ²)					
min	11.3	11.6	9.5	1.2	62.3
max	1440.8	5718.2	1884.6	652.3	11 716.5
N					
min	2	1	1	1	4
max	11	22	20	15	19

Location of sampling: F: The Forest of Obihiro; H: natural forest preservation of Hokkaido Obihiro Agricultural High School; R: Urikari River; T: Tokachi Ecology Park; U: Obihiro University of Agriculture and Veterinary Medicine. A_{shoot} : total leaf area of each shoot (cm²); N : total leaf number of each shoot.

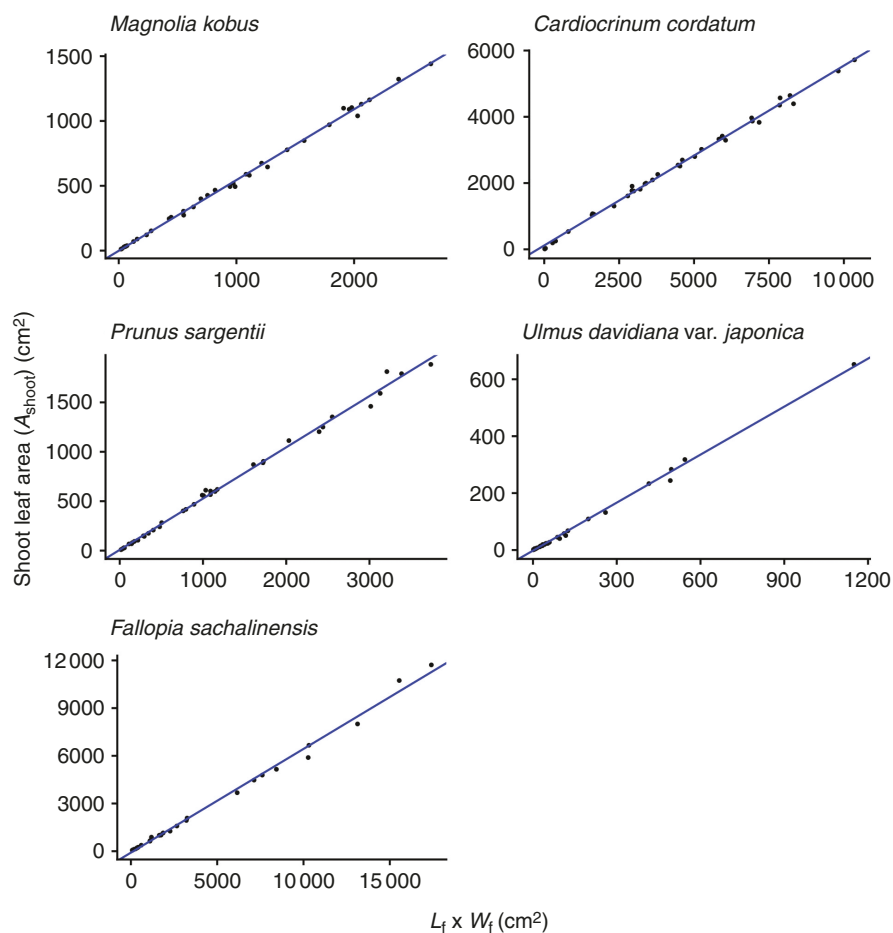


FIG. 3. The total leaf area of a shoot (A_{shoot}) is proportional to the product of foliage length (L_f) and width (W_f), as predicted by eqn (4). Each closed circle indicates an individual shoot. See Fig. 2B for the definition of foliage length and width. The blue lines show OLS (ordinary least squares) regression lines ($R^2 > 0.994$). See Table 2 for the regression results.

in a cool-temperate region of Japan, and were within 10 km from the Obihiro Weather Station (42°52'N 143°10'E, altitude: 76 m a.s.l.). Mean annual temperature and precipitation at the weather station during 1998–2017 were 7.2 °C and 937 mm, respectively (Japan Meteorological Agency, 2020). Shoots

with obvious damage (e.g. leaf loss due to herbivory etc.) were excluded. For the woody species, shoots that had sylleptic shoots (i.e. branching within the current year) were not sampled. Our sampling strategy was not random, but instead the shoots were sampled to cover a wide range sizes within each

TABLE 2. Results of the regression analyses (OLS: ordinary least squares; SMA: standardized major axis). All regressions are significant ($P < 1.0 \times 10^{-5}$ for all cases).

$Y = a + bX$		Type		Mgk	Cac	Prs	Udj	Fas
Y	X							
A_{shoot}	$L_f \times W_f$ $\left\{ \begin{array}{l} L_f \equiv \sum_{\text{shoot}} W_{\text{leaf}} \\ W_f \equiv \max_{\text{shoot}} (L_{\text{leaf}}) \end{array} \right.$	OLS	a	-1.492	117.352	7.904	-2.109	-90.461
			b	0.546	0.543	0.519	0.562	0.652
			R^2	0.997	0.996	0.996	0.997	0.994
$\log_{10}(A_{\text{shoot}})$	$\log_{10} W_f$ $= \log_{10} \left[\max_{\text{shoot}} (L_{\text{leaf}}) \right]$	OLS	a	-1.135	-1.758	-1.620	-0.565	-0.065
			b	3.088	3.554	3.682	2.647	2.511
			R^2	0.976	0.957	0.966	0.951	0.944
$\log_{10}(A_{\text{shoot}})$	$\log_{10} \left[\max_{\text{shoot}} (W_{\text{leaf}}) \right]$	SMA	a	-1.178	-1.866	-1.690	-0.606	-0.151
			b	3.125	3.630	3.745	2.712	2.582
			R^2	0.977	0.958	0.967	0.953	0.946
$\log_{10}(A_{\text{shoot}})$	$\log_{10} \left[\max_{\text{shoot}} (W_{\text{leaf}}) \right]$	OLS	a	-0.350	-0.502	-0.603	-0.199	-0.598
			b	3.084	2.841	3.654	3.064	3.111
			R^2	0.963	0.930	0.946	0.956	0.967
$\log_{10}(A_{\text{shoot}})$	$\log_{10} W_f$	SMA	a	-0.402	-0.635	-0.687	-0.228	-0.657
			b	3.141	2.943	3.754	3.132	3.162
			R^2	0.964	0.932	0.947	0.957	0.968
$\log_{10} L_f$	$\log_{10} W_f$	SMA	a	-0.939	-1.783	-1.387	-0.415	0.090
			$b (= \beta)$	2.187	2.856	2.806	1.892	1.629
			R^2	0.961	0.916	0.939	0.907	0.909
$\log_{10}(A_{\text{shoot}})$	$\log_{10} N$	OLS	a	0.742	1.853	0.830	0.333	0.103
			b	2.325	1.443	1.865	1.980	3.137
			R^2	0.963	0.857	0.946	0.855	0.922
A_{shoot}	$N \cdot \max_{\text{shoot}} (A_{\text{leaf}})$	SMA	a	0.711	1.747	0.785	0.271	-0.013
			$b (= \alpha)$	2.368	1.555	1.916	2.136	3.263
			R^2	0.964	0.861	0.948	0.859	0.925
$\log_{10} \left(\frac{A_{\text{shoot}}}{W_f} \right)$	$\log_{10} N$	OLS	a	24.144	420.913	33.972	-4.077	-97.621
			b	0.630	0.369	0.637	0.690	0.712
			R^2	0.980	0.976	0.987	0.996	0.989
$\log_{10} \left(\frac{A_{\text{shoot}}}{W_f} \right)$	$\log_{10} N$	OLS	a	0.111	0.796	0.137	-0.029	-0.065
			b	1.605	1.080	1.390	1.288	1.997
			R^2	0.977	0.896	0.962	0.871	0.943
A_{shoot}	$N \left[\frac{\min_{\text{shoot}} (A_{\text{leaf}}) + \max_{\text{shoot}} (A_{\text{leaf}})}{2} \right]$	SMA	a	0.097	0.740	0.114	-0.064	-0.118
			$b (= \gamma)$	1.623	1.139	1.416	1.378	2.054
			R^2	0.977	0.899	0.963	0.874	0.945
A_{shoot}	$N \left[\frac{\min_{\text{shoot}} (A_{\text{leaf}}) + \max_{\text{shoot}} (A_{\text{leaf}})}{2} \right]$	OLS	a	7.376	310.017	-16.200	-5.339	-122.219
			$b (= k)$	1.092	0.758	1.109	1.193	1.221
			R^2	0.994	0.981	0.991	0.992	0.993
A_{leaf}	$L_{\text{leaf}} \cdot W_{\text{leaf}}$	OLS	a	1.163	-	-0.799	0.121	1.514
			b	0.648	-	0.643	0.663	0.798
			R^2	0.989	-	0.992	0.992	0.992

Mgk: *Magnolia kobus*; Cac: *Cardiocrinum cordatum*; Prs: *Prunus sargentii*; Udj: *Ulmus davidiana* var. *japonica*; Fas: *Fallopia sachalinensis*.

species (i.e. small, medium and large shoots were intentionally selected). Because healthy shoots were selected based solely on their sizes, both shaded and well-lit shoots were sampled for trees. For herbaceous species (*Cardiocrinum* and *Fallopia*), all shoots (ramets) within the same species grew in similar environments in their natural habitats. *Cardiocrinum* were sampled in partially shaded forest understories or small gaps and *Fallopia* were sampled in open clearings. For *Cardiocrinum*, leaf sizes were measured non-destructively *in situ* (see below). For the other species, shoots were harvested using pruning scissors or a long-reach pruner, sometimes with the aid of a stepladder. Immediately after sampling, shoots were stored in closed plastic bags with wet paper towels to avoid desiccation.

Scanning (described below) was conducted within the same sampling day.

Leaf size measurements

Leaf length (L_{leaf}) is defined as the length of the leaf lamina, measured from the lamina tip to the point at which the lamina attaches to the petiole. Leaf width (W_{leaf}) is defined as the maximum lamina width perpendicular to the midvein. Individual leaf area (A_{leaf}) is defined as the area of one side of each lamina (John *et al.*, 2017). For *Cardiocrinum*, we measured L_{leaf} and W_{leaf} of all leaves on each stem using a

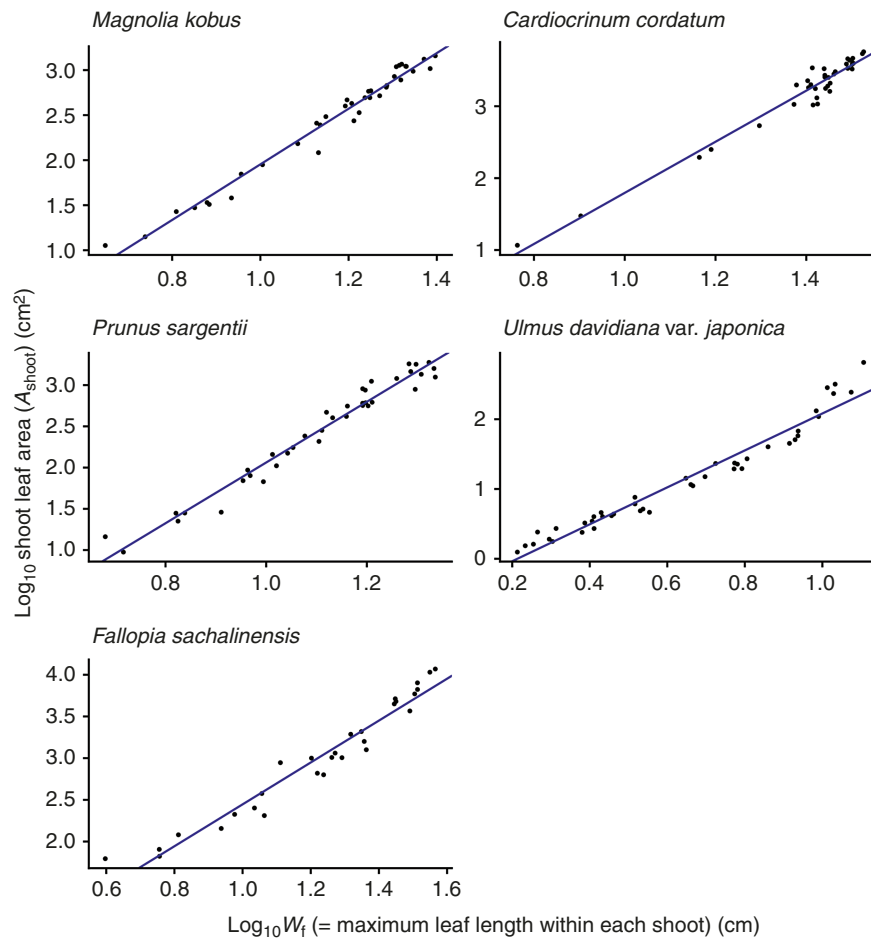


FIG. 4. The total leaf area of a shoot (A_{shoot}) is a power function of foliage width (W_f), defined as the maximum individual leaf length of the shoot, as predicted by eqn (6). Each closed circle indicates one individual shoot. The blue lines show the OLS (ordinary least squares) regression lines ($R^2 = 0.944\text{--}0.976$). See Table 2 for the regression results.

measuring tape *in situ*. Then, A_{leaf} for this species was estimated using the following equation: individual leaf area = 0.7169 (leaf length \times width) (Koyama *et al.*, 2012). For the other species, the harvested leaves were scanned using flatbed digital scanners (LiDE 210, Canon, Tokyo, Japan, 400 dpi; or 400-SCN025, Sanwa Supply, Okayama, Japan, 600 dpi). The sizes (L_{leaf} , W_{leaf} , A_{leaf}) of each leaf were measured using ImageJ v.1.50i or 1.53a (Schneider *et al.*, 2012). For *Cardiocrinum*, both reproductive (large bolting plants) and vegetative shoots (rosettes) were sampled to cover the natural size range of this species, and the flower buds on top of *Cardiocrinum* stems were excluded as leaves. No reproductive organs were found among the sampled shoots of the other species. Some large shoots of *Prunus* and *Ulmus* trees, and most of the shoots of the erect herb *Fallopia*, were still elongating at the time of harvesting (June–August). For these shoots, only leaves of which laminae were unfolded (even when they were young and still expanding) were counted and measured; small folded immature leaves or leaf primordia near or at the shoot apical meristem were excluded as leaves. Among large shoots of *Fallopia*, small leaves were occasionally found on small lateral shoots that were branched from the main stem. These

small lateral shoots were not measured because we focused on a single stem in this study. The total amount of those immature and lateral leaves was small compared to the total amount of leaves on the main stem.

All statistical analyses were performed with the statistical software R v.4.1.0 (R Core Team, 2021) and the packages *cowplot* (Wilke, 2016), *ggplot2* (Wickham, 2016), *gridExtra* (Auguie, 2017) and *smatr* (Warton *et al.*, 2012). Following Warton *et al.* (2006), ordinary least squares (OLS) and/or standardized major axis (SMA) regression analyses were performed for each relationship. OLS lines were fitted to predict variable Y (e.g. A_{shoot}) from X (e.g. $L_f \times W_f$) with the R function *lm*. SMA lines were fitted to determine the mutual allometric relationship between two variables (e.g. foliage length vs. width) with the *sma* function of the package *smatr*. The R^2 values of the OLS lines reported in this article were adjusted.

RESULTS

For all species investigated, the foliage length-times-width equation (eqn 4) explains A_{shoot} with high accuracy ($R^2 > 0.994$ for all species; Fig. 3; Table 2). As predicted by

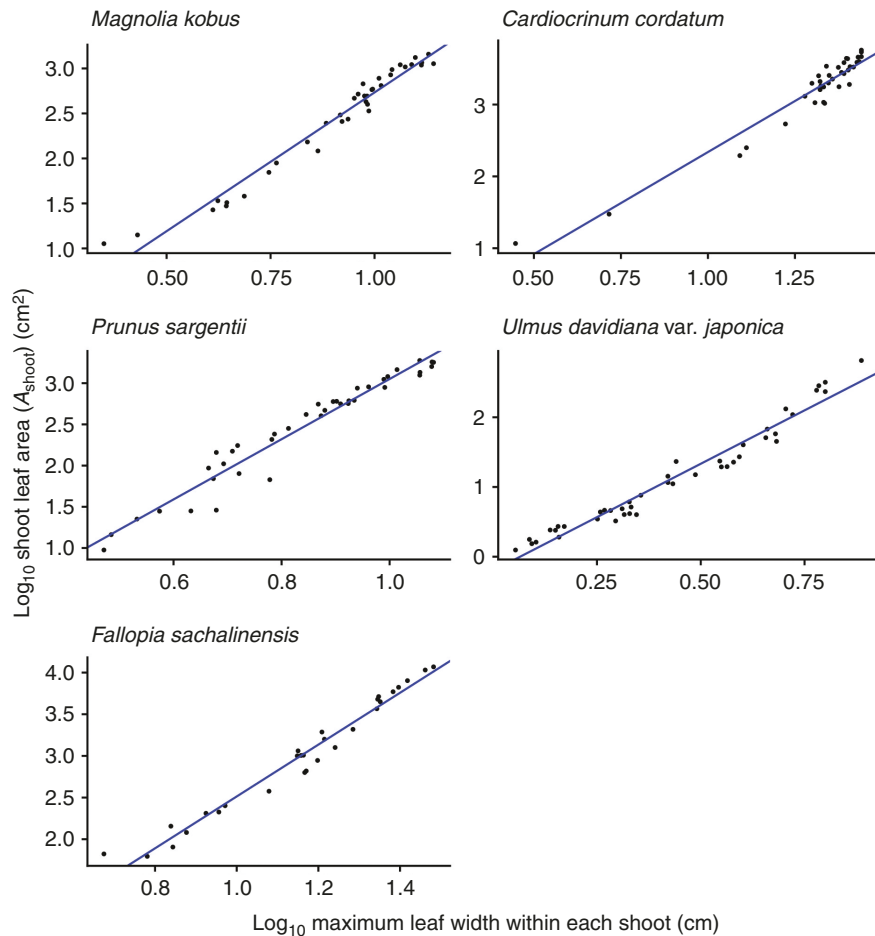


FIG. 5. The total leaf area of a shoot (A_{shoot}) is a power function of the maximum individual leaf width of the shoot, as predicted by eqn (7). Each closed circle indicates an individual shoot. The blue lines show the OLS (ordinary least squares) regression lines ($R^2 = 0.930\text{--}0.967$). See Table 2 for the regression results.

Eqns (6) and (7), A_{shoot} can also be predicted as an allometric equation of maximum leaf length (i.e. foliage width W_f ; Fig. 4; Table 2) or maximum leaf width alone (Fig. 5; Table 2), though with less accuracy (OLS: $R^2 = 0.930\text{--}0.976$; SMA: $0.932\text{--}0.977$). The allometric relationship between foliage width and length (eqn 5) was also supported ($R^2 = 0.905\text{--}0.960$; Fig. 6; Table 2). As expected, the scaling exponent β was >1 , and the value of β varied greatly among the species (Table 2).

As predicted by eqn (9), A_{shoot} is expressed as a power function of the total number of leaves on that shoot (N) with the SMA regression exponents >1 (Fig. 7; Table 2), though for this relationship substantial deviations from the regression lines ($R^2 = 0.859\text{--}0.964$; Table 2) were observed in the region for $N \leq 3$ ($\log_{10} N \leq 0.48$). This is especially evident when $N = 1$, in which case A_{shoot} is represented by only a single leaf, and as N increases, the values of A_{shoot} become stable as they are calculated as the sum of many leaves. The present data also reconfirm all previously known empirical relationships found by Sun *et al.* [eqn (8); $R^2 > 0.976$; Fig. 8; Table 2], by Heerema–Spann–Teobaldelli *et al.* [eqn (12); OLS: $R^2 = 0.871\text{--}0.977$; SMA: $R^2 = 0.874\text{--}0.977$; Fig. 9; Table 2] and by Lopes–Pinto [eqn (13); $R^2 > 0.981$; Fig. 10;

Table 2]. The present data also reconfirm the leaf-level relationships that individual leaf area is proportional to the product of its lamina length and width [eqn (2); $R^2 > 0.989$; Table 2].

DISCUSSION

Leaf vs. shoot elongation

The structure of a shoot, including size variation and arrangement of leaves, determines the light-harvesting efficiency of plants (Givnish, 1984; Valladares and Brites, 2004; Pearcy *et al.*, 2005; Smith *et al.*, 2017; Olson *et al.*, 2018; Koyama *et al.*, 2020; Iwabe *et al.*, 2021). If a shoot is to minimize the cost of current light harvesting, the optimal solution derived by Givnish (1982) is to have a single large leaf with no investment in the stem (i.e. no stem elongation). Why does a shoot have multiple leaves instead of a single large leaf? There are mutually non-exclusive explanations for the benefit of producing multi-leaved stems rather than single-leaved stems. First, plants are subject to competition with neighbours (Givnish, 1982; Anten, 2016), and existing leaves will be gradually shaded by neighbouring plants in the future. Under competition, plants should continuously elongate their

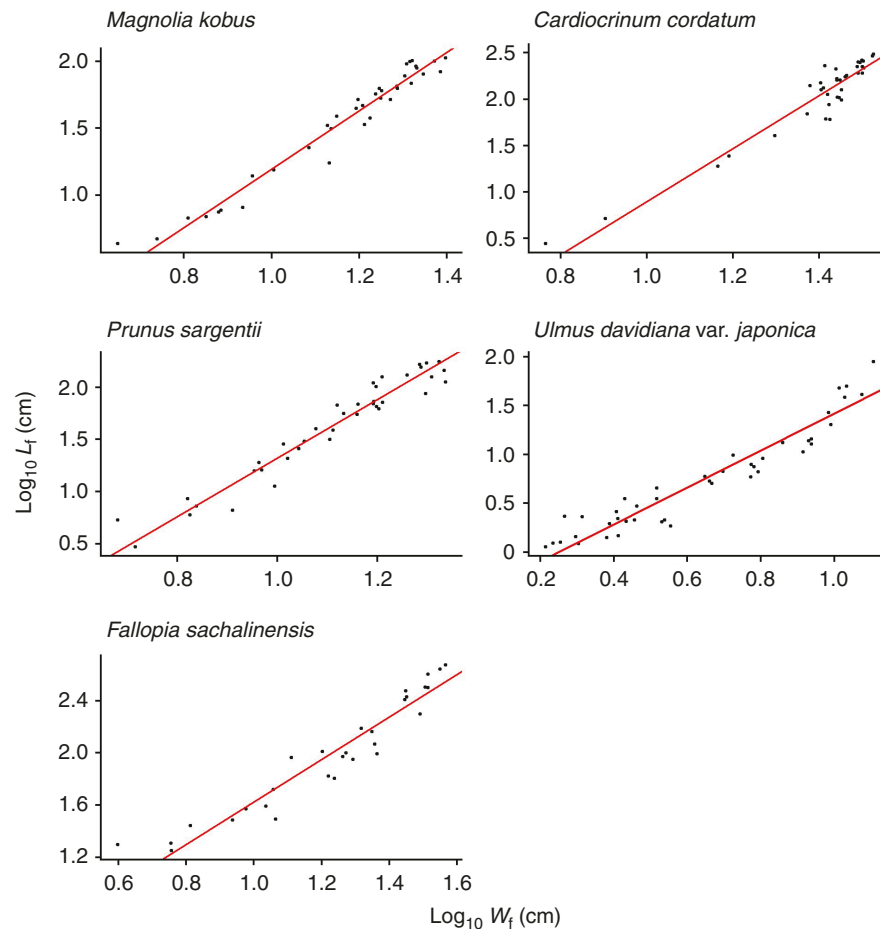


FIG. 6. Log–log linear (allometric) relationship between foliage length (L_f) and width (W_f). The regression slopes correspond to β in eqn (5). Each closed circle indicates an individual shoot. The red lines show the SMA (standardized major axis) regression lines ($R^2 = 0.905\text{--}0.960$). See Table 2 for the regression results.

stems and produce new leaves in better-lit positions (Koyama and Kikuzawa, 2009; Anten, 2016; Koyama *et al.*, 2020). Therefore, a shoot has at least two functions in terms of light capture: current light harvesting and space acquisition, the latter of which contributes to future light harvesting (Yagi and Kikuzawa, 1999; Sterck *et al.*, 2005; Laurans and Vincent, 2016; Koyama *et al.*, 2020). Differentiation of short vs. long shoots can be considered as a continuum of a strategy along the trade-off between these two functions (Yagi and Kikuzawa, 1999). In the present dataset, the exponent β was >1 [eqn (5); Table 2], indicating that larger foliage had a larger foliage length relative to its foliage width, as expected because larger foliage consists of more leaves than smaller foliage (Fig. 7). This phenomenon is called geometric dissimilitude and it can be considered as a shift in strategy along size variation (Niklas, 1994; Okie, 2013). These results are consistent with the observation that long shoots are specialized for space acquisition whereas short shoots are specialized for light capture, and there is a continuous shift between these two extremes (Yagi and Kikuzawa, 1999). Second, larger leaves produce a thicker boundary layer that reduces heat and gas exchange (Schuepp, 1993; Xu *et al.*, 2009); therefore, larger leaves are subject to greater heat stress (Vogel, 2009). Having compound leaves that

consist of multiple leaflets instead of simple large leaves can effectively reduce the boundary layer resistance (Gurevitch and Schuepp, 1990; Xu *et al.*, 2009). At the level of individual leaves, Schrader *et al.* (2021) demonstrated that the length-times-width equation (eqn 2) is valid for compound leaves. However, at the shoot level, leaf shape (e.g. simple vs. compound) may also affect the leaf–shoot allometric relationship (Yang *et al.*, 2009). Therefore, the scaling relationships may also be affected by the leaf shape, which is in turn affected by the environment (Royer *et al.*, 2005; Xu *et al.*, 2009). Third, Kleiman and Aarssen (2007) suggested that producing more leaves, instead of fewer but larger ones, is more beneficial because it allows stems to have more buds and eventually leads to greater lateral growth and higher plasticity of allocation between growth and reproduction. Fourth, for a given limit on the total leaf area of a shoot, larger leaves incur a disproportionately greater cost of supporting tissues (Niinemets *et al.*, 2007; Shi *et al.*, 2020). Fifth, if a plant has many leaves, then the feeding or attacking efficiency of herbivores or pathogens may be reduced (Brown *et al.*, 1991). Altogether, the observed variation of β across the five species may reflect these multiple compounding factors. Therefore, further investigations on species with different leaf shapes (such as compound leaves), leaf

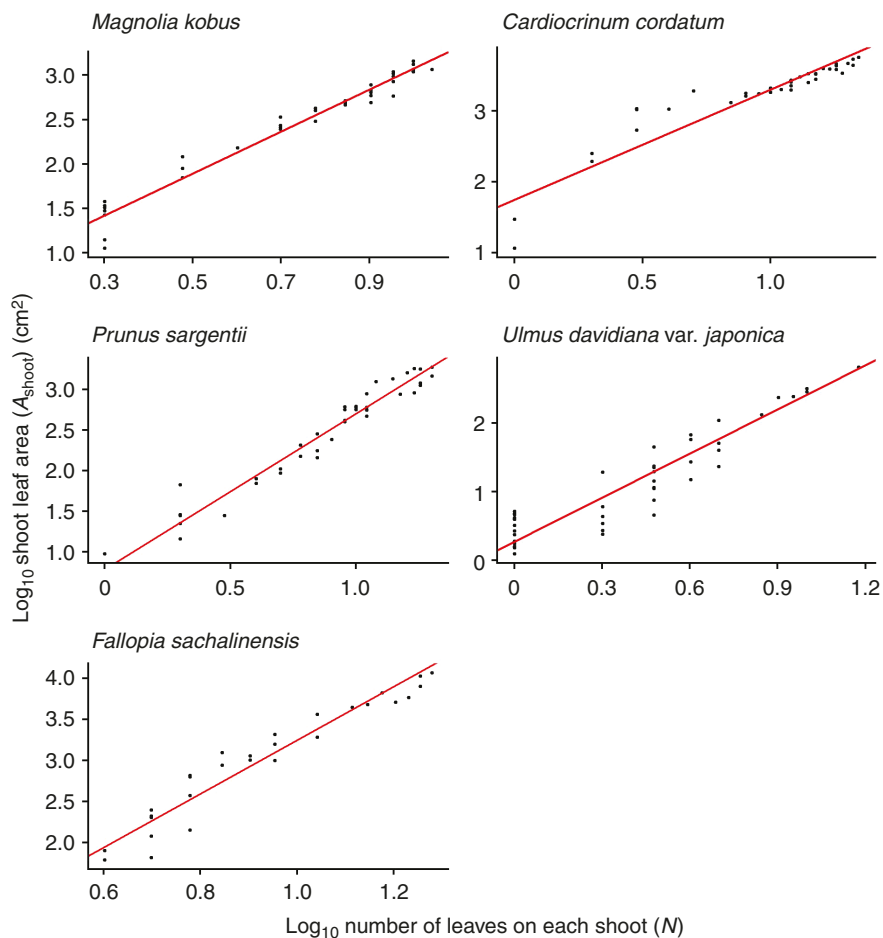


FIG. 7. Log–log linear (allometric) relationship between the total leaf area of a shoot (A_{shoot}) and the total number of leaves on the shoot (N). The regression slopes correspond to α in eqn (9). Each closed circle indicates one individual shoot. The red lines show the SMA (standardized major axis) regression lines ($R^2 = 0.859$ – 0.964). See Table 2 for the regression results.

sizes, leafing intensities and environments (including herbivores and pathogens) are needed.

In this study, we intentionally ignored the 3D arrangement of foliage and instead considered the 2D structure of foliage as being analogous to a single large leaf (Fig. 2B). By doing so, our length-times-width equation successfully predicted A_{shoot} with high accuracy without considering any details of the actual foliage structure other than size. The simplification applied in this study is in contrast to existing models, which consider the 3D arrangement of leaves, such as phyllotaxis (Valladares and Brites, 2004; Smith *et al.*, 2017), internode length (Meng *et al.*, 2013), stem inclination angle (Meng *et al.*, 2013), and the resultant light interception and within-shoot self-shading (Valladares and Brites, 2004; Koyama and Kikuzawa, 2010; Smith *et al.*, 2017; Olson *et al.*, 2018). Our model does not consider stem traits, such as cross-sectional area (Brouat *et al.*, 1998; Yan *et al.*, 2013; Smith *et al.*, 2017; Lehnbach *et al.*, 2018; Sun *et al.*, 2019a, b, 2020; Fajardo *et al.*, 2020), length-to-diameter ratio (Xiang *et al.*, 2009a, Levionnois *et al.*, 2021), conduit size, which determines hydraulic efficiency (Savage *et al.*, 2010; Chen *et al.*, 2012; Fan *et al.*, 2017; Trueba *et al.*, 2019; Olson *et al.*, 2020;

Bortolami *et al.*, 2021; Levionnois *et al.*, 2021), stem mechanical properties (Brouat and McKey, 2001; Chen *et al.*, 2009; Trueba *et al.*, 2016; Fan *et al.*, 2017; Olson *et al.*, 2018; Baer *et al.*, 2021; Levionnois *et al.*, 2021) or the associated stem construction costs (Yang *et al.*, 2010; Givnish, 2020). Nonetheless, because our model focuses only on a population of leaf laminae, it is not mutually exclusive to the previous models. Instead, the geometric property of foliage can be incorporated to improve the previous models, which do not consider the within-shoot size variation of individual leaves.

Limitations of the model

The product of leaf lamina length and width can predict individual leaf area, and this relationship holds for diverse taxa and for different growth conditions, without considering the underlying leaf structures such as venation (Blonder *et al.*, 2020; Kawai and Okada, 2020), lobation (Schuepp, 1993; Kusi and Karsai, 2020), lamina folding (Fleck *et al.*, 2003; Deguchi and Koyama, 2020), epidermal features (Maslova *et al.*, 2021) and internal mesophyll structures (Oguchi *et al.*, 2005), all of

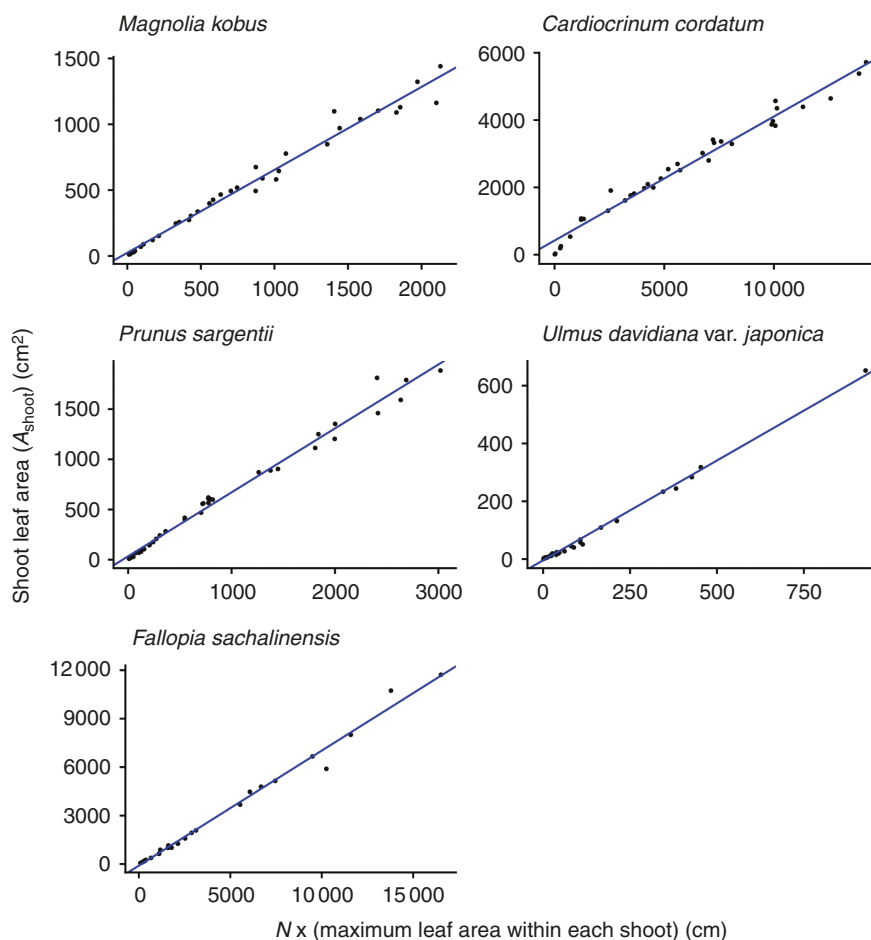


FIG. 8. The total leaf area of a shoot (A_{shoot}) is proportional to the product of the maximum individual leaf area and the number of leaves on the shoot (N), as predicted by eqn (8). Each closed circle indicates one individual shoot. The blue lines show the OLS (ordinary least squares) regression lines ($R^2 > 0.976$).

which are known to differ among angiosperm species and under different environmental conditions. The consistency of the shoot-level results among eudicots, Magnoliids and monocots obtained herein may imply that the present results may also be generalized across angiosperms, as is the case for individual leaves. However, because our aim was to propose and test a new model as a starting point, we chose only five typical temperate woody and herbaceous species. In general, leaf–shoot allometric relationships are affected by climate or altitude (Westoby and Wright, 2003; Sun *et al.*, 2006, 2019a; Xiang *et al.*, 2009a, b, 2010; Zhu *et al.*, 2019), as well as by leaf habit (i.e. deciduous vs. evergreen) (Brouat *et al.*, 1998; Yang *et al.*, 2008, 2009; Milla, 2009; Zhu *et al.*, 2019; Fajardo *et al.*, 2020). Therefore, it remains unclear whether the present results can be applied to different situations, including other species from extreme climates or different life forms, such as evergreen conifers. Additionally, our model does not consider compound leaves. At the level of individual leaves, a recent study demonstrated that the length-times-width equation (eqn 2) is valid for both simple and compound leaves (Schrader *et al.*, 2021). However, at the level of shoots, leaf shape may also affect the leaf–shoot allometric relationship (Yang *et al.*, 2009). Therefore, more comprehensive datasets that include a diversity of leaf forms are needed to validate our model. Furthermore, our

model does not consider the reproductive organs. The scaling relationships between reproductive organs and shoot size has long been recognized (Chen *et al.*, 2009; Scott and Aarssen, 2013; Miranda *et al.*, 2019), and the existence of reproductive organs also alters scaling relationship among vegetative organs (Fajardo *et al.*, 2020). Therefore, future studies are needed to elucidate whether the simple relationship found in the present study is affected by the existence of reproductive organs.

CONCLUSIONS

Based on the geometric properties of foliage, we proposed the ‘foliage length-times-width equation’ that accurately predicts the total leaf area of a shoot. The model unifies several previously established empirical relationships into a single theory. We also demonstrated that the total leaf area of a shoot can also be predicted by maximum individual leaf lamina length or width alone. The dataset of five species from diverse taxa generally supported the model predictions, though deviations from the model were also observed. More comprehensive datasets that include a diversity of species are needed to test the generality of our model in future studies.

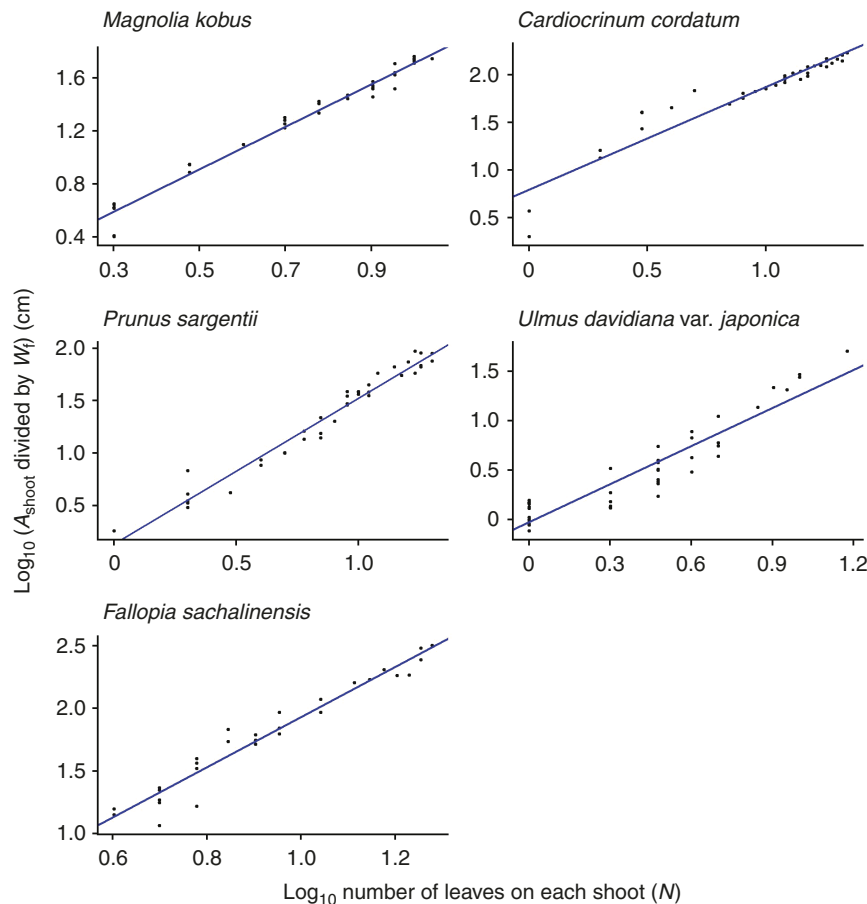


Fig. 9. The total leaf area of a shoot divided by foliage width (A_{shoot}/W_f) is a power function of the number of leaves on the shoot (N). The regression slopes correspond to γ in eqn (12). Each closed circle indicates an individual shoot. The blue lines show the OLS (ordinary least squares) regression lines ($R^2 = 0.871\text{--}0.977$). See Table 2 for the regression results.

ACKNOWLEDGEMENTS

We thank staff members of the Obihiro City Office, Obihiro Forest Hagukumu, the Hokkaido Obihiro Agricultural High School, the Tokachi Ecology Park Foundation, and the Field Center of Animal Science and Agriculture of the Obihiro University of Agriculture and Veterinary Medicine for providing permission for fieldwork at the study sites. The authors declare no conflicts of interest. K.K. designed the study, proposed the mathematical model and conducted the fieldwork. K.K. and D.D.S. wrote the manuscript. All the data, including the scanned digital images of leaves, are available from the Dryad Digital Repository: doi: 10.5061/dryad.sxksn035r

FUNDING

K.K. was funded by the Japan Society for the Promotion of Science (KAKENHI grant numbers 18K06406, 19H02987). D.D.S. was supported by National Science Foundation DEB-1557906.

LITERATURE CITED

- Ackerly DD, Bazzaz FA. 1995. Leaf dynamics, self-shading and carbon gain in seedlings of a tropical pioneer tree. *Oecologia* **101**: 289–298. doi:10.1007/BF00328814.
- Ackerly DD, Donoghue MJ. 1998. Leaf size, sapling allometry, and Corner's rules: phylogeny and correlated evolution in maples (*Acer*). *The American Naturalist* **152**: 767–791. doi:10.1086/286208.
- Anten NPR. 2016. Optimization and game theory in canopy models. In: Hikosaka K, Niinemets Ü, Anten NPR, eds. *Canopy photosynthesis: from basics to applications*. Dordrecht: Springer Netherlands, 355–377.
- APG IV. 2016. An update of the Angiosperm Phylogeny Group classification for the orders and families of flowering plants: APG IV. *Botanical Journal of the Linnean Society* **181**: 1–20.
- Augie B. 2017. <https://CRAN.R-project.org/package=gridExtra>.
- Baer AB, Fickle JC, Medina J, Robles C, Pratt RB, Jacobsen AL. 2021. Xylem biomechanics, water storage, and density within roots and shoots of an angiosperm tree species. *Journal of Experimental Botany* **72**: 7984–7997.
- Banavar JR, Cooke TJ, Rinaldo A, Maritan A. 2014. Form, function, and evolution of living organisms. *Proceedings of the National Academy of Sciences of the United States of America* **111**: 3332–3337. doi:10.1073/pnas.1401336111.
- Bazzaz FA, Harper JL. 1977. Demographic analysis of the growth of *Linum usitatissimum*. *New Phytologist* **78**: 193–208. doi:10.1111/j.1469-8137.1977.tb01558.x.
- Bentley LP, Stegen JC, Savage VM, et al. 2013. An empirical assessment of tree branching networks and implications for plant allometric scaling models. *Ecology Letters* **16**: 1069–1078. doi:10.1111/ele.12127.
- Blonder B, Both S, Jodra M, et al. 2020. Linking functional traits to multiscale statistics of leaf venation networks. *New Phytologist* **228**: 1796–1810.
- Bortolami G, Farolfi E, Badel E, et al. 2021. Seasonal and long-term consequences of esca grapevine disease on stem xylem integrity. *Journal of Experimental Botany* **72**: 3914–3928.
- Brouat C, Gibernau M, Amsellem L, McKey D. 1998. Corner's rules revisited: ontogenetic and interspecific patterns in leaf–stem allometry. *New Phytologist* **139**: 459–470.

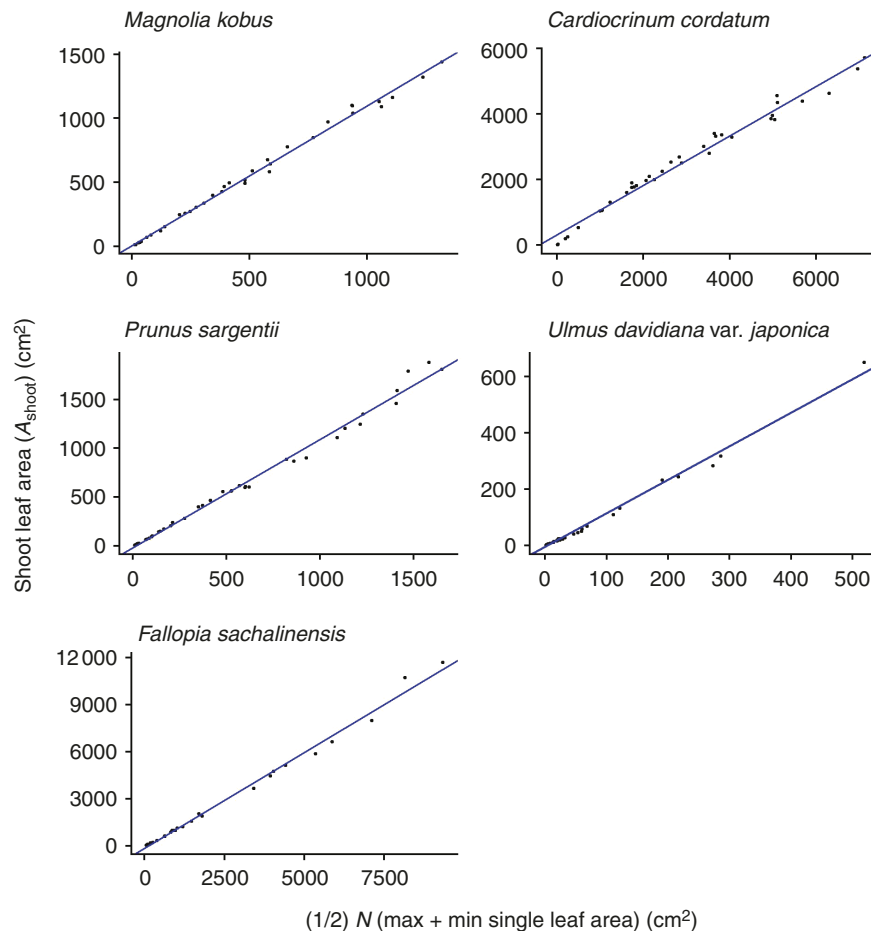


FIG. 10. The total leaf area of a shoot (A_{shoot}) is proportional to the product of the number of leaves (N) times (maximum + minimum individual leaf area) divided by 2. The regression slopes correspond to k in eqn (13). Each closed circle indicates an individual shoot. The blue lines show the OLS (ordinary least squares) regression lines ($R^2 > 0.981$). See Table 2 for the regression results.

- Brouat C, McKey D. 2001.** Leaf-stem allometry, hollow stems, and the evolution of caulinary domatia in myrmecophytes. *New Phytologist* **151**: 391–406.
- Brown VK, Lawton JH, Grubb PJ, Chaloner WG, Harper JL, Lawton JH. 1991.** Herbivory and the evolution of leaf size and shape. *Philosophical Transactions of the Royal Society of London, Series B: Biological Sciences* **333**: 265–272.
- Bultynck L, Ter Steege MW, Schortemeyer M, Poot P, Lambers H. 2004.** From individual leaf elongation to whole shoot leaf area expansion: a comparison of three *Aegilops* and two *Triticum* species. *Annals of Botany* **94**: 99–108.
- Cain SA, Castro GDO. 1959.** *Manual of vegetation analysis*. New York: Harper & Brothers.
- Chen H, Niklas KJ, Sun S. 2012.** Testing the packing rule across the twig-petiole interface of temperate woody species. *Trees* **26**: 1737–1745.
- Chen H, Niklas KJ, Yang D, Sun S. 2009.** The effect of twig architecture and seed number on seed size variation in subtropical woody species. *New Phytologist* **183**: 1212–1221.
- Corner EJH. 1949.** The durian theory or the origin of the modern tree. *Annals of Botany* **13**: 367–414.
- Deguchi R, Koyama K. 2020.** Photosynthetic and morphological acclimation to high and low light environments in *Petasites japonicus* subsp. *giganteus*. *Forests* **11**: 1365.
- DeJong TM, Day KR, Johnson RS. 1989.** Partitioning of leaf nitrogen with respect to within canopy light exposure and nitrogen availability in peach (*Prunus persica*). *Trees-Structure and Function* **3**: 89–95.
- Dombroskie SL, Aarssen LW. 2012.** The leaf size/number trade-off within species and within plants for woody angiosperms. *Plant Ecology and Evolution* **145**: 38–45.
- Dombroskie SL, Tracey AJ, Aarssen LW. 2016.** Leafing intensity and the fruit size/number trade-off in woody angiosperms. *Journal of Ecology* **104**: 1759–1767.
- Enquist BJ, West GB, Brown JH. 2009.** Extensions and evaluations of a general quantitative theory of forest structure and dynamics. *Proceedings of the National Academy of Sciences of the United States of America* **106**: 7046–7051.
- Fajardo A, Mora JP, Robert E. 2020.** Corner's rules pass the test of time: little effect of phenology on leaf-shoot and other scaling relationships. *Annals of Botany* **126**: 1129–1139.
- Falconer K. 2003.** *Fractal geometry: mathematical foundations and applications*, 2nd edn. Chichester: John Wiley & Sons.
- Fan Z-X, Sterck F, Zhang S-B, Fu P-L, Hao G-Y. 2017.** Tradeoff between stem hydraulic efficiency and mechanical strength affects leaf-stem allometry in 28 *Ficus* tree species. *Frontiers in Plant Science* **8**: 1619.
- Field C. 1983.** Allocating leaf nitrogen for the maximization of carbon gain - leaf age as a control on the allocation program. *Oecologia* **56**: 341–347.
- Field CB. 1991.** Ecological scaling of carbon gain to stress and resource availability. In: Mooney HA, Winner WE, Pell EJ, eds. *Response of plants to multiple stresses*. San Diego: Academic Press, 35–65.
- Fleck S, Niinemets U, Cescatti A, Tenhunen JD. 2003.** Three-dimensional lamina architecture alters light-harvesting efficiency in *Fagus*: a leaf-scale analysis. *Tree Physiology* **23**: 577–589.
- Givnish T. 1984.** Leaf and canopy adaptations in tropical forests. In: Medina E, Mooney HA, Vázquez-Yanes C, eds. *Physiological ecology of plants of the wet tropics*. Dordrecht: Springer, 51–84.
- Givnish TJ. 1982.** On the adaptive significance of leaf height in forest herbs. *The American Naturalist* **120**: 353–381.
- Givnish TJ. 2020.** The adaptive geometry of trees revisited. *The American Naturalist* **195**: 935–947.

- Gurevitch J, Schuepp PH. 1990. Boundary layer properties of highly dissected leaves: an investigation using an electrochemical fluid tunnel. *Plant, Cell & Environment* **13**: 783–792.
- Harper JL, Bell AD. 1979. The population dynamics of growth form in organisms with modular construction. In: Anderson RM, Turner BD, Taylor LR, eds. *Population dynamics* 20th symposium British ecological society. Oxford, UK: Blackwell Publishing, 29–52.
- Heerema R, Weinbaum S, Pernice F, Dejong T. 2008. Spur survival and return bloom in almond [*Prunus dulcis* (Mill.) DA Webb] varied with spur fruit load, specific leaf weight, and leaf area. *The Journal of Horticultural Science and Biotechnology* **83**: 274–281.
- Hikosaka K, Kumagai To, Ito A. 2016. Modeling canopy photosynthesis. In: Hikosaka K, Niinemets Ü, Anten NPR, eds. *Canopy photosynthesis: from basics to applications*. Dordrecht: Springer Netherlands, 239–268.
- Huang L, Niinemets U, Ma J, Schrader J, Wang R, Shi P. 2021. Plant age has a minor effect on non-destructive leaf area calculations in Moso Bamboo (*Phyllostachys edulis*). *Symmetry* **13**: 369.
- Huang W, Su X, Ratkowsky DA, Niklas KJ, Gielis J, Shi P. 2019. The scaling relationships of leaf biomass vs. leaf surface area of 12 bamboo species. *Global Ecology and Conservation* **20**: e00793.
- Huxley JS. 1932. *Problems of relative growth*. London: Methuen.
- Iwabe R, Koyama K, Komamura R. 2021. Shade avoidance and light foraging of a clonal woody species, *Pachysandra terminalis*. *Plants* **10**: 809.
- Japan Meteorological Agency. 2020. <https://www.jma.go.jp>. Accessed 14 September 2020.
- John GP, Scoffoni C, Buckley TN, Villar R, Poorter H, Sack L. 2017. The anatomical and compositional basis of leaf mass per area. *Ecology Letters* **20**: 412–425.
- Kawai K, Okada N. 2020. Leaf vascular architecture in temperate dicotyledons: correlations and link to functional traits. *Planta* **251**: 17.
- Kleiman D, Aarssen LW. 2007. The leaf size/number trade-off in trees. *Journal of Ecology* **95**: 376–382.
- Komamura R, Koyama K, Yamauchi T, Konno Y, Gu L. 2021. Pollination contribution differs among insects visiting *Cardiocrinum cordatum* flowers. *Forests* **12**: 452.
- Koyama K, Hidaka Y, Ushio M. 2012. Dynamic scaling in the growth of a non-branching plant, *Cardiocrinum cordatum*. *PLoS One* **7**: e45317.
- Koyama K, Kikuzawa K. 2009. Is whole-plant photosynthetic rate proportional to leaf area? A test of scalings and a logistic equation by leaf demography census. *American Naturalist* **173**: 640–649.
- Koyama K, Kikuzawa K. 2010. Geometrical similarity analysis of photosynthetic light response curves, light saturation and light use efficiency. *Oecologia* **164**: 53–63.
- Koyama K, Shirakawa H, Kikuzawa K. 2020. Redeployment of shoots into better-lit positions within the crowns of saplings of five species with different growth patterns. *Forests* **11**: 1301.
- Koyama K, Yamamoto K, Ushio M. 2017. A lognormal distribution of the lengths of terminal twigs on self-similar branches of elm trees. *Proceedings of the Royal Society B: Biological Sciences* **284**: 20162395.
- Kurosawa Y, Mori S, Wang M, et al. 2021. Initial burst of root development with decreasing respiratory carbon cost in *Fagus crenata* Blume seedlings. *Plant Species Biology* **36**: 146–156.
- Kusi J, Karsai I. 2020. Plastic leaf morphology in three species of *Quercus*: The more exposed leaves are smaller, more lobated and denser. *Plant Species Biology* **35**: 24–37.
- Laurans M, Vincent G. 2016. Are inter- and intraspecific variations of sapling crown traits consistent with a strategy promoting light capture in tropical moist forest? *Annals of Botany* **118**: 983–996.
- Lecigne B, Delagrangue S, Taugourdeau O. 2021. Annual shoot segmentation and physiological age classification from tIs data in trees with acrotonic growth. *Forests* **12**: 391.
- Lehnebach R, Beyer R, Letort V, Heuret P. 2018. The pipe model theory half a century on: a review. *Annals of Botany* **121**: 773–795.
- Levionnois S, Salmon C, Alméras T, et al. 2021. Anatomies, vascular architectures, and mechanics underlying the leaf size-stem size spectrum in 42 Neotropical tree species. *Journal of Experimental Botany* **72**: 7957–7969.
- Li Y, Niklas KJ, Gielis J, et al. 2021. An elliptical blade is not a true ellipse, but a superellipse—evidence from two *Michelia* species. *Journal of Forestry Research*.
- Lin S, Niklas KJ, Wan Y, et al. 2020. Leaf shape influences the scaling of leaf dry mass vs. area: a test case using bamboos. *Annals of Forest Science* **77**: 11.
- Lopes C, Pinto P. 2005. Easy and accurate estimation of grapevine leaf area with simple mathematical models. *Vitis* **44**: 55–61.
- Maslova NP, Karasev EV, Xu S-L, et al. 2021. Variations in morphological and epidermal features of shade and sun leaves of two species: *Quercus bambusifolia* and *Q. myrsinifolia*. *American Journal of Botany* **108**: 1441–1463.
- Meng F, Cao R, Yang D, Niklas KJ, Sun S. 2013. Within-twig leaf distribution patterns differ among plant life-forms in a subtropical Chinese forest. *Tree Physiology* **33**: 753–762.
- Milla R. 2009. The leafing intensity premium hypothesis tested across clades, growth forms and altitudes. *Journal of Ecology* **97**: 972–983.
- Miranda J, Finley J, Aarssen L. 2019. Leafing intensity predicts fecundity allocation in herbaceous angiosperms. *Folia Geobotanica* **54**: 191–198.
- Mori S, Yamaji K, Ishida A, et al. 2010. Mixed-power scaling of whole-plant respiration from seedlings to giant trees. *Proceedings of the National Academy of Sciences of the United States of America* **107**: 1447–1451.
- Niinemets Ü. 2016. Within-canopy variations in functional leaf traits: structural, chemical and ecological controls and diversity of responses. In: Hikosaka K, Niinemets Ü, Anten NPR, eds. *Canopy photosynthesis: from basics to applications*. Dordrecht: Springer Netherlands, 101–141.
- Niinemets U, Portsmouth A, Tena D, Tobias M, Matesanz S, Valladares F. 2007. Do we underestimate the importance of leaf size in plant economics? Disproportional scaling of support costs within the spectrum of leaf physiognomy. *Annals of Botany* **100**: 283–303.
- Niklas KJ. 1994. *Plant allometry: The scaling of form and process*. Chicago: University of Chicago Press.
- Niklas KJ, Enquist BJ. 2001. Invariant scaling relationships for interspecific plant biomass production rates and body size. *Proceedings of the National Academy of Sciences* **98**: 2922–2927.
- Niklas KJ, Enquist BJ. 2002. On the vegetative biomass partitioning of seed plant leaves, stems, and roots. *The American Naturalist* **159**: 482–497.
- Ogawa K. 2008. The leaf mass/number trade-off of Kleiman and Aarssen implies constancy of leaf biomass, its density and carbon uptake in forest stands: scaling up from shoot to stand level. *Journal of Ecology* **96**: 188–191.
- Ogawa K, Furukawa A, Hagihara A, Abdullah AM, Awang M. 1995. Morphological and phenological characteristics of leaf development of *Durio zibethinus* Murray (Bombacaceae). *Journal of Plant Research* **108**: 511–515.
- Oguchi R, Hikosaka K, Hirose T. 2005. Leaf anatomy as a constraint for photosynthetic acclimation: differential responses in leaf anatomy to increasing growth irradiance among three deciduous trees. *Plant Cell and Environment* **28**: 916–927.
- Ohara M, Narumi T, Yoshizane T, Okayasu T, Masuda J, Kawano S. 2006. *7: Cardiocrinum cordatum* (Thunb.) Makino (Liliaceae). *Plant Species Biology* **21**: 201–207.
- Okie JG. 2013. General models for the spectra of surface area scaling strategies of cells and organisms: fractality, geometric dissimilitude, and internalization. *American Naturalist* **181**: 421–439.
- Olson M, Rosell JA, Martínez-Pérez C, et al. 2020. Xylem vessel-diameter–shoot-length scaling: ecological significance of porosity types and other traits. *Ecological Monographs* **90**: e01410.
- Olson ME, Aguirre-Hernández R, Rosell JA. 2009. Universal foliage-stem scaling across environments and species in dicot trees: plasticity, biomechanics and Corner's Rules. *Ecology Letters* **12**: 210–219.
- Olson ME, Rosell JA, Zamora Muñoz S, Castorena M. 2018. Carbon limitation, stem growth rate and the biomechanical cause of Corner's rules. *Annals of Botany* **122**: 583–592.
- Pearcy RW, Muraoka H, Valladares F. 2005. Crown architecture in sun and shade environments: assessing function and trade-offs with a three-dimensional simulation model. *New Phytologist* **166**: 791–800.
- Phinopoulos V, Cadima J, Lopes C. 2015. Estimation of leaf area in grapevine cv. Syrah using empirical models. In: 19th International Meeting of Viticulture GiESCO, Peach Rouge-Montpellier, 31 May–5 June, 2015, vol. 1, 385–388: GiESCO.
- R Core Team. 2021. *R: a language and environment for statistical computing*. Vienna: R Foundation for Statistical Computing.
- Royer DL, Wilf P, Janesko DA, Kowalski EA, Dilcher DL. 2005. Correlations of climate and plant ecology to leaf size and shape: potential proxies for the fossil record. *American Journal of Botany* **92**: 1141–1151.
- Savage VM, Bentley LP, Enquist BJ, et al. 2010. Hydraulic trade-offs and space filling enable better predictions of vascular structure and function in plants. *Proceedings of the National Academy of Sciences of the United States of America* **107**: 22722–22727.

- Schneider CA, Rasband WS, Eliceiri KW. 2012. NIH Image to ImageJ: 25 years of image analysis. *Nature Methods* 9: 671–675.
- Schrader J, Shi P, Royer DL, et al. 2021. Leaf size estimation based on leaf length, width and shape. *Annals of Botany* 128: 395–406.
- Schuepp PH. 1993. Tansley Review No. 59 Leaf boundary layers. *New Phytologist* 125: 477–507.
- Scott SL, Aarssen LW. 2012. Within-species leaf size–number trade-offs in herbaceous angiosperms. *Botany* 90: 223–235.
- Scott SL, Aarssen LW. 2013. Leaf size versus leaf number trade-offs in dioecious angiosperms. *Journal of Plant Ecology* 6: 29–35.
- Seleznyova AN, Greer DH. 2001. Effects of temperature and leaf position on leaf area expansion of kiwifruit (*Actinidia deliciosa*) shoots: development of a modelling framework. *Annals of Botany* 88: 605–615.
- Shi P-J, Li Y-R, Niinemets U, Olson E, Schrader J. 2021a. Influence of leaf shape on the scaling of leaf surface area and length in bamboo plants. *Trees* 35: 709–715.
- Shi P, Li Y, Hui C, Ratkowsky DA, Yu X, Niinemets U. 2020. Does the law of diminishing returns in leaf scaling apply to vines? – Evidence from 12 species of climbing plants. *Global Ecology and Conservation* 21: e00830.
- Shi P, Yu K, Niinemets U, Gielis J. 2021b. Can leaf shape be represented by the ratio of leaf width to length? Evidence from nine species of *Magnolia* and *Michelia* (Magnoliaceae). *Forests* 12: 41.
- Shinozaki K, Yoda K, Hozumi K, Kira T. 1964. A quantitative analysis of plant form—the pipe model theory: I. Basic analyses. *Japanese Journal of Ecology* 14: 97–105.
- Smith DD, Sperry JS, Adler FR. 2017. Convergence in leaf size versus twig leaf area scaling: do plants optimize leaf area partitioning? *Annals of Botany* 119: 447–456.
- Spann TM, Heerema RJ. 2010. A simple method for non-destructive estimation of total shoot leaf area in tree fruit crops. *Scientia Horticulturae* 125: 528–533.
- Sterck FJ, Schieving F. 2007. 3-D growth patterns of trees: effects of carbon economy, meristem activity, and selection. *Ecological Monographs* 77: 405–420.
- Sterck FJ, Schieving F, Lemmens A, Pons TL. 2005. Performance of trees in forest canopies: explorations with a bottom-up functional–structural plant growth model. *New Phytologist* 166: 827–843.
- Sun J, Chen X, Wang M, Li J, Zhong Q, Cheng D. 2020. Application of leaf size and leafing intensity scaling across subtropical trees. *Ecology and Evolution* 10: 13395–13402.
- Sun J, Fan R, Niklas KJ, et al. 2017. ‘Diminishing returns’ in the scaling of leaf area vs. dry mass in Wuyi Mountain bamboos, Southeast China. *American Journal of Botany* 104: 993–998.
- Sun J, Wang M, Lyu M, et al. 2019a. Stem and leaf growth rates define the leaf size vs. number trade-off. *AoB PLANTS* 11: plz063.
- Sun J, Wang M, Lyu M, et al. 2019b. Stem diameter (and not length) limits twig leaf biomass. *Frontiers in Plant Science* 10: 185.
- Sun S, Jin D, Shi P. 2006. The leaf size–twig size spectrum of temperate woody species along an altitudinal gradient: an invariant allometric scaling relationship. *Annals of Botany* 97: 97–107.
- Sun S, Niklas Karl J, Fang F, Xiang S, Wu X, Yang X. 2010. Is branching intensity interspecifically related to biomass allocation? A survey of 25 dicot shrub species from an open-growing dry valley. *International Journal of Plant Sciences* 171: 615–625.
- Teobaldelli M, Basile B, Giuffrida F, et al. 2019a. Analysis of cultivar-specific variability in size-related leaf traits and modeling of single leaf area in three medicinal and aromatic plants: *Ocimum basilicum* L., *Mentha* spp., and *Salvia* spp. *Plants* 9: 13.
- Teobaldelli M, Roupael Y, Fascella G, Cristofori V, Rivera CM, Basile B. 2019b. Developing an accurate and fast non-destructive single leaf area model for loquat (*Eriobotrya japonica* Lindl) cultivars. *Plants* 8: 230.
- Teobaldelli M, Roupael Y, Gonnella M, et al. 2020. Developing a fast and accurate model to estimate allometrically the total shoot leaf area in grapevines. *Scientia Horticulturae* 259: 108794.
- Trueba S, Delzon S, Isnard S, Lens F. 2019. Similar hydraulic efficiency and safety across vesselless angiosperms and vessel-bearing species with scalariform perforation plates. *Journal of Experimental Botany* 70: 3227–3240.
- Trueba S, Isnard S, Barthélémy D, Olson ME. 2016. Trait coordination, mechanical behaviour and growth form plasticity of *Amborella trichopoda* under variation in canopy openness. *AoB PLANTS* 8: plw068.
- Valladares F, Brites D. 2004. Leaf phyllotaxis: Does it really affect light capture? *Plant Ecology* 174: 11–17.
- Vogel S. 2009. Leaves in the lowest and highest winds: temperature, force and shape. *New Phytologist* 183: 13–26.
- Wang M, Mori S, Kurosawa Y, Ferrio JP, Yamaji K, Koyama K. 2021. Consistent scaling of whole-shoot respiration between Moso bamboo (*Phyllostachys pubescens*) and trees. *Journal of Plant Research* 134: 989–997.
- Warton DI, Duursma RA, Falster DS, Taskinen S. 2012. smatr 3 – an R package for estimation and inference about allometric lines. *Methods in Ecology and Evolution* 3: 257–259.
- Warton DI, Wright IJ, Falster DS, Westoby M. 2006. Bivariate line-fitting methods for allometry. *Biological Reviews* 81: 259–291.
- West GB, Enquist BJ, Brown JH. 2009. A general quantitative theory of forest structure and dynamics. *Proceedings of the National Academy of Sciences of the United States of America* 106: 7040–7045.
- Westoby M, Wright IJ. 2003. The leaf size – twig size spectrum and its relationship to other important spectra of variation among species. *Oecologia* 135: 621–628.
- White PS. 1983. Corner’s rules in eastern deciduous trees: allometry and its implications for the adaptive architecture of trees. *Bulletin of the Torrey Botanical Club* 110: 203–212.
- Whitman T, Aarssen LW. 2010. The leaf size/number trade-off in herbaceous angiosperms. *Journal of Plant Ecology* 3: 49–58.
- Wickham H. 2016. *ggplot2: elegant graphics for data analysis*. Cham: Springer International Publishing.
- Wilke CO. 2016. *cowplot: streamlined plot theme and plot annotations for ‘ggplot2’*. CRAN Repos 2: R2.
- Xiang S, Liu Y, Fang F, Wu N, Sun S. 2009a. Stem architectural effect on leaf size, leaf number, and leaf mass fraction in plant twigs of woody species. *International Journal of Plant Sciences* 170: 999–1008.
- Xiang S, Wu N, Sun S. 2009b. Within-twig biomass allocation in subtropical evergreen broad-leaved species along an altitudinal gradient: allometric scaling analysis. *Trees* 23: 637–647.
- Xiang S, Wu N, Sun S. 2010. Testing the generality of the ‘leafing intensity premium’ hypothesis in temperate broad-leaved forests: a survey of variation in leaf size within and between habitats. *Evolutionary Ecology* 24: 685–701.
- Xu F, Guo W, Xu W, Wei Y, Wang R. 2009. Leaf morphology correlates with water and light availability: What consequences for simple and compound leaves? *Progress in Natural Science* 19: 1789–1798.
- Yagi T, Kikuzawa K. 1999. Patterns in size-related variations in current-year shoot structure in eight deciduous tree species. *Journal of Plant Research* 112: 343–352.
- Yan E-R, Wang X-H, Chang SX, He F. 2013. Scaling relationships among twig size, leaf size and leafing intensity in a successional series of subtropical forests. *Tree Physiology* 33: 609–617.
- Yang D, Li G, Sun S. 2008. The generality of leaf size versus number trade-off in temperate woody species. *Annals of Botany* 102: 623–629.
- Yang D, Li G, Sun S. 2009. The effects of leaf size, leaf habit, and leaf form on leaf/stem relationships in plant twigs of temperate woody species. *Journal of Vegetation Science* 20: 359–366.
- Yang D, Niklas KJ, Xiang S, Sun S. 2010. Size-dependent leaf area ratio in plant twigs: implication for leaf size optimization. *Annals of Botany* 105: 71–77.
- Yu X, Shi P, Schrader J, Niklas KJ. 2020. Nondestructive estimation of leaf area for 15 species of vines with different leaf shapes. *American Journal of Botany* 107: 1481–1490.
- Zhu G, Niklas KJ, Li M, et al. 2019. ‘Diminishing Returns’ in the scaling between leaf area and twig size in three forest communities along an elevation gradient of Wuyi Mountain, China. *Forests* 10: 1138.

APPENDIX

Derivation of eqn (8)

When different-sized foliage sets are affine to each other, they become congruent (i.e. identical in shape) when normalized to the same size. This indicates that the maximum leaf length (or width) within each shoot relative to the mean value of the same shoot is constant, leading to the following relationships:

$$\begin{cases} \text{mean}_{\text{shoot}} (L_{\text{leaf}}) \propto \max_{\text{shoot}} (L_{\text{leaf}}) \\ \text{mean}_{\text{shoot}} (W_{\text{leaf}}) \propto \max_{\text{shoot}} (W_{\text{leaf}}) \end{cases} \quad (14)$$

By taking the product of both sides of the two lines in eqn (14), and using eqn (2), we obtained:

$$\text{mean}_{\text{shoot}} (A_{\text{leaf}}) \propto \max_{\text{shoot}} (A_{\text{leaf}}) \quad (15)$$

In deriving eqn (15), we assumed that the leaf that has maximum (or mean) length within each shoot also has the maximum (or mean) width in the same shoot. By multiplying both sides of eqn (15) by the total number of leaves on each shoot (N), we obtained:

$$N \cdot \text{mean}_{\text{shoot}} (A_{\text{leaf}}) \propto N \cdot \max_{\text{shoot}} (A_{\text{leaf}}) \quad (16)$$

Because the left-hand-side of eqn (16) is A_{shoot} , we obtained eqn (8).

Derivation of eqn (9)

In this section, we assume that lamina length and width of an individual leaf are approximately proportional to each other (Ogawa *et al.*, 1995), and that individual leaf area can be predicted as the quadratic function of either leaf length or width alone (Teobaldelli *et al.*, 2019a, b):

$$A_{\text{leaf}} \propto (L_{\text{leaf}})^2 \quad (17)$$

Equation (17) can also be used to predict the maximum A_{leaf} within each shoot:

$$\max_{\text{shoot}} (A_{\text{leaf}}) \propto \left[\max_{\text{shoot}} (L_{\text{leaf}}) \right]^2 \quad (18)$$

By multiplying both sides of eqn (18) by the total number of leaves on each shoot (N), we obtained:

$$N \cdot \max_{\text{shoot}} (A_{\text{leaf}}) \propto N \cdot \left[\max_{\text{shoot}} (L_{\text{leaf}}) \right]^2 \quad (19)$$

By combining eqns (8) and (19), we obtained:

$$A_{\text{shoot}} \propto N \cdot \left[\max_{\text{shoot}} (L_{\text{leaf}}) \right]^2 \quad (20)$$

By using our definition of W_f (eqn 3), eqn (20) can be rewritten as follows:

$$A_{\text{shoot}} \propto N \cdot W_f^2 \quad (21)$$

By combining eqns (6) and (21), we obtained:

$$W_f^{\beta+1} \propto N \cdot W_f^2 \quad (22)$$

Equation (22) can be solved for W_f :

$$W_f \propto N^{\frac{1}{\beta-1}} \quad (23)$$

By substituting eqn (23) into eqn (6), we obtained:

$$A_{\text{shoot}} \propto N^{\frac{\beta+1}{\beta-1}} \equiv N^\alpha \quad (24)$$

Derivation of eqn (10)

Equation (9) can be solved for N_f :

$$N \propto A_{\text{shoot}}^{\frac{1}{\alpha}} \quad (25)$$

Using eqn (25), we obtained:

$$\frac{A_{\text{shoot}}}{N} \propto (A_{\text{shoot}})^{1-\frac{1}{\alpha}} \equiv (A_{\text{shoot}})^\lambda \quad (26)$$

Derivation of eqn (11)

By combining eqns (5) and (23), we obtained:

$$L_f \propto W_f^\beta \propto N^{\frac{\beta}{\beta-1}} \quad (27)$$

By substituting eqn (27) into eqn (4), we obtained:

$$A_{\text{shoot}} \propto W_f \cdot N^{\frac{\beta}{\beta-1}} \equiv W_f \cdot N^\gamma \quad (28)$$

Derivation of eqn (13)

When different-sized foliage sets are affine to each other, the maximum leaf size relative to the mean value and the minimum leaf size relative to the mean value would be constants, independent of foliage size. This leads to the following relationship:

$$\text{mean}_{\text{shoot}} (A_{\text{leaf}}) \propto \min_{\text{shoot}} (A_{\text{leaf}}) \quad (29)$$

By dividing both sides of eqns (15) and (29) by 2, and adding them, we obtained:

$$\text{mean}_{\text{shoot}} (A_{\text{leaf}}) \propto \frac{\min_{\text{shoot}} (A_{\text{leaf}}) + \max_{\text{shoot}} (A_{\text{leaf}})}{2} \quad (30)$$

By multiplying both sides of eqn (30) by N , we obtained eqn (13).